

3D β -induced changes in the edge region of the Large Helical Device

The three-dimensional (3D) plasma response to the magnetic field structure is studied for high- β plasmas in the Large Helical Device (LHD). The radial electric field E_r is measured in the peripheral region. A positive electric field appears in this region and suggests the boundary between opened and closed field lines. The transition to positive E_r always takes place outside of the last closed flux surface (LCFS). 3D MHD modeling predicts the expansion of the effective plasma boundary due to the β -induced 3D plasma response. The position of the appearance of strong E_r is almost comparable to the expanded plasma boundary obtained via modeling. Thus, the predicted 3D plasma response has been measured by the change of sign of E_r in LHD experiments.

In these experiments, a volume-averaged beta (β) of 5% was achieved in the quasi-steady state [1]. For such high- β plasmas, changes in magnetic field structure are to be expected. Because the LHD magnetic field is an intrinsically 3D structure, the plasma current flowing along 3D field lines drives a perturbed magnetic field which can break the nested flux surfaces of the vacuum field; this is the so-called “3D plasma response.” Understanding the effects of the β -induced plasma current is an important and critical issue in stellarator and heliotron research. Understanding the nature of stochastic field lines is also a critical issue for application of the resonant magnetic perturbation (RMP) in tokamaks.

The 3D plasma response to the magnetic field has been studied theoretically and numerically. As the lowest order of the 3D plasma response, 3D MHD equilibrium was studied using a 3D MHD equilibrium calculation code without the assumption of nested flux surfaces [2, 3]. Figure 1 shows a Poincaré plot of magnetic field lines for the finite- β equilibrium obtained as a best fit to the experimental result in Ref. [1]. Profiles of the connection length L_C from equilibrium calculation and the electron tempera-

ture T_e from experimental results (shot 69910) are also shown for reference. The magnetic axis shifts from $R = 3.53$ m to about 3.8 m and magnetic field lines become stochastic, especially in the peripheral region. Despite the stochastic magnetic field lines, it appears that T_e spreads out into the peripheral region and a gradient of T_e exists in this region. Theory predicts that it may be possible to confine plasma on the stochastic field lines [3]. The mechanism for this is still a mystery.

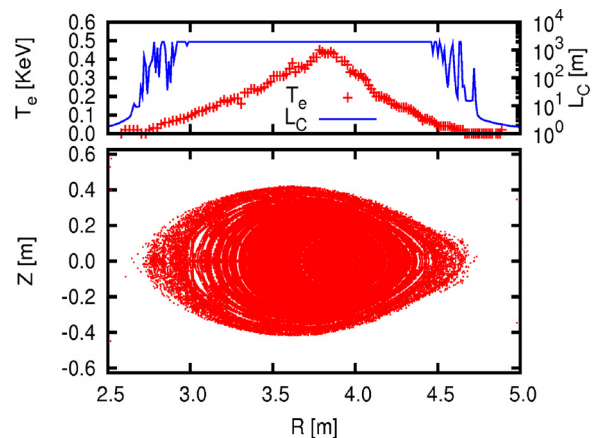


Fig. 1. A Poincaré plot of magnetic field lines for $\langle\beta\rangle \sim 4.8\%$ at the horizontal elongated cross section. Profiles of L_C and T_e (shot 69910) are also plotted for reference.

In this issue . . .

3D β -induced changes in the edge region of the Large Helical Device

3D MHD equilibrium analysis predicts an outward motion of the effective plasma boundary due to finite- β . The radial electric field E_r is measured in the peripheral region. Positive E_r in the edge region suggests the boundary between open and closed field lines. The transition to positive E_r always takes place outside the vacuum boundary. 1

Coordinated Working Group Meeting (CWGM11) for Stellarator-Heliotron Research

A summary of the meeting held 11–13, March 2013 at CIEMAT in Madrid, Spain, is presented. 5

To confirm the reason for the existence of ∇T_e on stochastic field lines, an experimental study to identify the magnetic field structure is necessary. However, few experimental studies of the 3D plasma response have been performed because identification of the magnetic field structure is difficult. Changes in magnetic field structure due to the 3D plasma response have been reported [4, 5, 6]. Recently, in the LHD experiment, identification of the magnetic field structure via measurement of E_r has been studied [7]. If electrons are lost along open field lines in a stochastic field, a positive E_r might appear to reduce the losses. This means that the appearance of positive E_r or strong shear in E_r suggests an “effective plasma boundary” between open and closed field lines. To test this suggestion, a comparison of the E_r measurement with 3D MHD equilibrium analysis, and identification of the magnetic field structure can be performed. Similar studies have been undertaken in tokamaks [8].

We first discuss changes of the effective plasma boundary due to the 3D plasma response. Next we report on studies of the change of the effective plasma boundary addressed using the E_r measurement. In particular, we study the relationship between the effective plasma boundary shift and increased β . Then the experimental observation is compared to the 3D MHD equilibrium analysis.

Analyses were done with the 3D MHD equilibrium code, HINT2 [2], which does not assume nested flux surfaces. Using HINT2, we can calculate the change of the topology of the magnetic field. Finally, we summarize this study.

In the LHD experiments, E_r is measured using a charge exchange recombination spectroscopy (CXRS) diagnostic [9]. The CXRS uses a charge-exchange recombination line of fully ionized carbon (the $n = 8-7$ transition of C VI) to measure the radial profiles of ion temperature T_i , density n_{C6+} , and toroidal and poloidal flow velocities V_ϕ and V_θ for carbon impurity ions. The radial electric field is defined by the following radial force balance equation:

$$E_r = (Z_j e n_j)^{-1} \nabla p_j - V_{\theta,j} B_\phi + V_{\phi,j} B_\theta. \quad (1)$$

Here, Z_j is the ion charge, n_j is the ion density, e is the magnitude of the electron charge, $p_j = n_j T_j$ is the ion pressure, with the ion temperature T_j . $V_{\theta,j}$ and $V_{\phi,j}$ are the ion poloidal and toroidal flow velocities, respectively, and B_θ and B_ϕ are the poloidal and toroidal magnetic fields, respectively. Details of the CXRS diagnostics are described in Ref. [9].

Profiles of V_ϕ , V_θ , E_r , and ∇E_r from a typical shot (109608, $t = 4.15$ s) are shown in Fig. 2. The volume-averaged beta $\langle \beta \rangle$ is about 1%. Profiles are plotted as a function of the effective plasma radius r_{eff} . The effective plasma radius is defined by the relation $S = \pi r_{\text{eff}}^2$, where S is averaged cross section on a best fitted MHD equilibrium

[10]. For reference, T_e and electron density n_e are also shown. The poloidal flow velocity V_θ increases rapidly in the peripheral region and E_r becomes positive in that region. Since the positive E_r in the peripheral region suggests lost electrons along open field lines, the position of $E_r = 0$ or strong E_r shear indicates the effective plasma boundary. In this case, the effective plasma boundary is at $r_{\text{eff}} \sim 0.55$ m. Note that ∇T_e still exists in the region $r_{\text{eff}} > 0.55$ m. However, 99% of total stored energy W_p lies within $r_{\text{eff}} \sim 0.55$ m, which means that the boundary identification based on E_r measurements is comparable to the that based on T_e and n_e measurements.

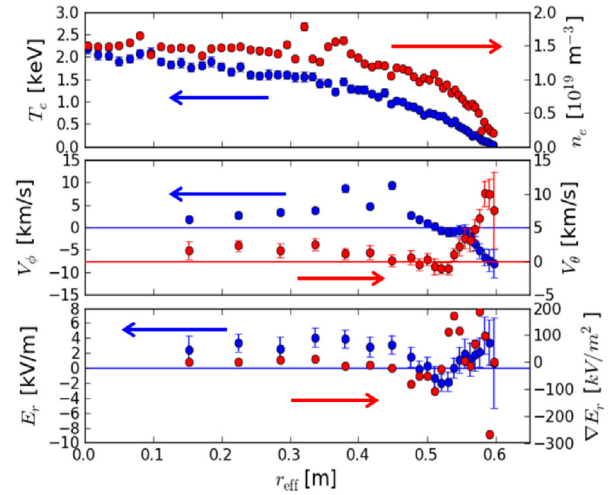


Fig. 2. Profiles of toroidal and poloidal flow velocities, V_ϕ and V_θ , the radial electric field E_r and shear of E_r for shot 109608 ($t = 4.15$ s). Those are plotted as a function of the effective minor radius r_{eff} . The volume-averaged beta $\langle \beta \rangle$ is about 1%. For reference, profiles of T_e and n_e are also shown.

Figure 3 shows the position of strong E_r shear as a function of $\langle \beta \rangle$. The blue and magenta horizontal lines indicate the position the vacuum LCFS ($R = 4.42$ m) and 20 cm outside the vacuum LCFS ($R = 4.62$ m), respectively.

For comparison, the position of the boundary containing 99% of W_p is also shown with green symbols. With increasing β , the magnetic field structure changes from its vacuum position; strong E_r shear also moves outward in R . For $\langle \beta \rangle \sim 3\%$, the position of strong E_r shear reaches $R \sim 4.6$ m. After this, the shift of strong E_r shear almost saturates. On the other hand, positions at which $W_p = 99\%$ become more scattered than the positions of strong E_r shear. This is not surprising because the calculation of the stored energy depends on the goodness of the 3D MHD equilibrium fit [10]. Thus, the identification of the effective plasma edge using E_r measurement is certain.

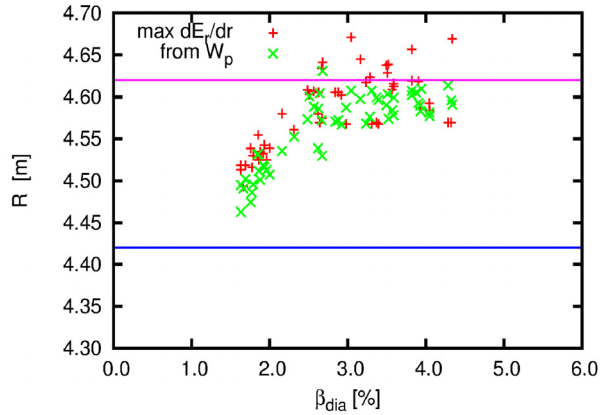


Fig. 3. Positions of strong E_r shear are shown as a function of $\langle\beta\rangle$ (red symbols). Horizontal lines in blue and magenta indicate the position of the vacuum LCFS ($R = 4.42$ m) and 20 cm outside of the vacuum LCFS ($R = 4.62$ m), respectively. Positions of the boundary containing 99% of W_p (green symbols) are also shown for comparison.

The E_r measurement shows a change in the boundary between open and closed field lines. Although strong E_r shear identifies only the position of the effective plasma boundary, it is difficult to identify the topology of the magnetic field with the present CXRS system. If we can measure E_r with finer resolution, it may be possible to identify the magnetic topology. If not, we need other diagnostics or techniques to identify the topology. One idea is heat pulse propagation experiments using modulated electron cyclotron heating (ECH) (MECH) [11]. In Ref. [11], the magnetic topology is clearly identified using heat pulse propagation. However, the MECH experiment is difficult at high β because the high- β experiment is done at low magnetic field strength (usually, $B < 1$ T). Also, there are no resonances in the peripheral region. Another idea is comparison with 3D modeling, which could reveal why the effective boundary changes due to increased β .

Figure 4 compares measured E_r and predictions from 3D MHD equilibrium analysis. Profiles are plotted for $\langle\beta\rangle \sim 1$ and 2%. On these figures, Poincaré plots of field lines calculated from the HINT2 code are also plotted at same poloidal cross section. In the plasma core, negative E_r appeared. This is comparable to the neoclassical transport predictions. However, in the peripheral region, positive E_r appeared. In addition, positions of strong E_r shear move to the outside of the torus due to increased β . In Fig. 4(a), the position of strong E_r shear moves about 5 cm from the LCFS. When compared to the HINT2 magnetic field structure, the position of strong E_r shear is almost same as the LCFS or slightly outward of the LCFS. On the other hand, in Fig. 4(b), the strong E_r shear position moves outward ~ 15 cm from the LCFS. For $\langle\beta\rangle \sim 2\%$, the stochastic

field line region is increased due to the 3D plasma response and is more expanded than in the $\langle\beta\rangle \sim 1\%$ case. However, although field lines become stochastic in the peripheral region, most field lines do not reach vessel wall and the connection length of open field lines L_C is still > 100 m. The electron mean free path is about 20–40 m. Therefore, from the viewpoint of transport, there is a possibility that the stochastic field line might retain plasma pressure, especially in the presence of E_r .

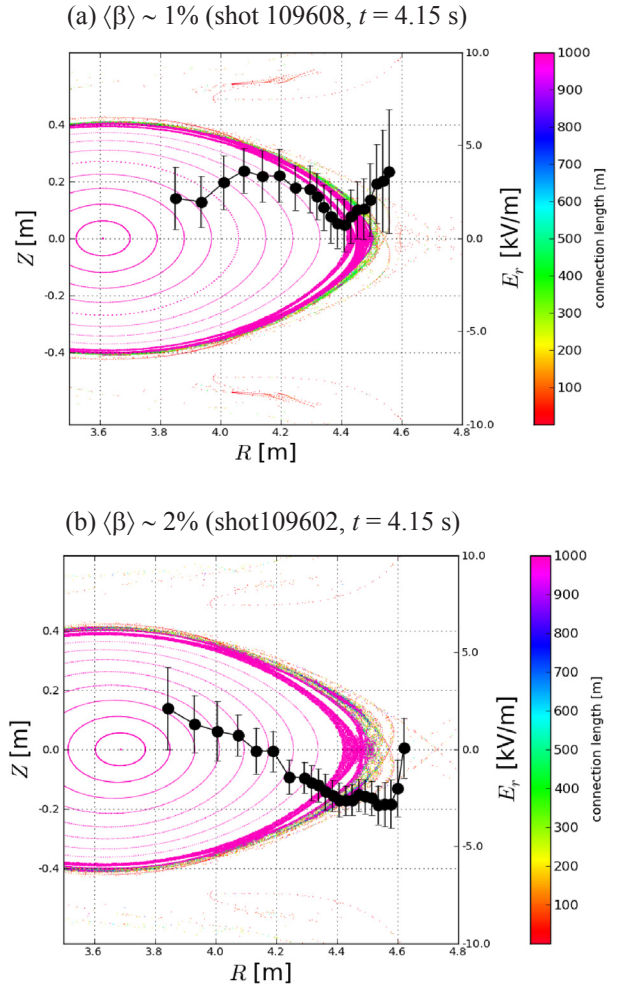


Fig. 4. Profiles of the poloidal rotation are plotted for $\langle\beta\rangle \sim 1\%$ and 2%, respectively. For reference, Poincaré plots are also shown at same poloidal cross section. In the Poincaré plots, only closed field lines ($L_C > 1000$ m) are plotted. Strong E_r shear appears at the boundary between closed and open field lines.

Conclusion

We studied the 3D plasma response to finite β by comparing measured E_r and results from a 3D MHD equilibrium analysis, paying special attention to changes in the effective plasma boundary. If magnetic field lines become stochastic and are open, a positive E_r appears in the

stochastic region. This behavior can be used to identify the effective plasma boundary. The change of the position of E_r or strong E_r shear with variation of β was examined. An increase in β or a strong E_r shear shift due to increased β shifts the LCFS outward. In comparison, the magnetic field structure calculated by HINT2 also shifts the LCFS outward due to the 3D plasma response, but the shift of the LCFS is not so large.

As an indicator of the 3D edge location, the edge of the plasma where the pressure is below 1% of the plasma pressure on the axis p_0 was studied. If magnetic field lines become stochastic, the connection length is still sufficiently long to keep a parallel pressure gradient. The change in the boundary location is correlated to the location of the development of strong E_r shear.

References

- [1] Sakakibara, S., et al., "MHD study of the reactor-relevant high-beta regime in the Large Helical Device," *Plasma Phys. Control. Fusion* **50** (2008) 124014.
- [2] Suzuki, Y., et al., "Development and application of HINT2 to helical system plasmas," *Nucl. Fusion* **46** (2006) L19.
- [3] Suzuki, Y., et al., "Effects of the Stochasticity on Transport Properties in High- β LHD," *Plasma Fusion Res.* **4** (2009) 036.
- [4] Hidalgo, C., et al., "Plasma fluctuations near the shear layer in the ATF torsatron," *Nucl. Fusion* **31** (1991) 1471.
- [5] Weller, A., et al., "Significance of MHD Effects in Stellarator Confinement," *Fusion Sci. Technol.* **50** (2006) 158.
- [6] Watanabe, K. Y., et al., "Change of plasma boundaries due to beta in heliotron plasma with helical divertor configuration," *Plasma Phys. Control. Fusion* **49** (2007) 605.
- [7] Kamiya, K., et al., "Characterization of edge radial electric field structures in Large Helical Device (LHD) and their viability of determination for the plasma boundary location," *Nucl. Fusion* **53** (2013) 013003.
- [8] Finken, K. H., et al., "Influence of the dynamic ergodic divertor on transport properties in TEXTOR," *Nucl. Fusion* **47** (2007) 522.
- [9] Yoshinuma, M., et al., "Charge-Exchange Spectroscopy with Pitch-Controlled Double-Slit Fiber Bundle on LHD," *Fusion Sci. Technol.* **58** (2010) 375.
- [10] Suzuki, C., et al., "Development and application of real-time magnetic coordinate mapping system in LHD," *Plasma Phys. Control. Fusion.* (2012) in press.
- [11] Ida, K., et al., "Bifurcation Phenomena of a Magnetic Island at a Rational Surface in a Magnetic-Shear Control Experiment," *Phys. Rev. Lett.* **100** (2008) 045003.

Yasuhiro Suzuki
National Institute for Fusion Science
Toki 509-5292, Japan
Graduate University for Advanced Studies SOKENDAI,
Toki 509-5292, Japan
E-mail: suzuki.yasuhiro@lhd.nifs.ac.jp

Coordinated Working Group Meeting (CWGM11) for Stellarator-Heliotron Research

The 11th Coordinated Working Group Meeting (CWGM11) was held 11–13, March 2013 at CIEMAT in Madrid, Spain. In addition to local participation, representatives of the following organizations (listed alphabetically by country) participated in the discussion: IPP-Greifswald (Germany), NIFS, Kyoto University (Japan), Kharkov (Ukraine), PPPL and University of Wisconsin-Madison (USA). The materials presented at the 11th CWGM are available at

<http://ishcdb.nifs.ac.jp/>

and

http://fusionwiki.ciemat.es/wikiCoordinated_Working_Group

(→ CWGM11).

A summary of the meeting follows.

C. Hidalgo (CIEMAT) opened with a welcoming address, in which he mentioned the successful evolution of the CWGM activity for the promotion of programmatic international collaboration towards systematic understanding, and its contribution to the world-wide fusion development.

The meeting was composed of 10 sessions as follows:

Flows and viscosity

This session was launched at the previous CWGM (Greifswald, 6–8 June 2012). The evolution since then and this year's plans across several helical devices were introduced. Simulation code verification and validation efforts (to be reported at the International Stellarator-Heliotron Workshop [ISHW]) are under way utilizing experimental data from LHD, TJ-II, W7-AS, and HSX. Extensions to the standard neoclassical assumptions, such as the non-local approach, the nonmonoenergetic treatment, and the inclusion of $\mathbf{E} \times \mathbf{B}$ flow compressibility, will be emphasized owing to the capabilities of the FORTEC-3D code.

Bias experiments in four helical devices in Japan (Tohoku University Helicac, CHS, Heliotron-J [H-J], and LHD) were reviewed. The required induced torque appears to increase as the effective ripple increases based on comparison among these devices. The international collaboration is valuable to extend the database. In this regard, the bias experiment in TJ-II was discussed. It was pointed out that the “iota window” for H-mode transitions in helical plasmas (observed in W7-AS, H-J and TJ-II) should be kept in mind as an extension of such bias experiments.

Isotope effects and multiscale physics were considered based on experimental findings in TJ-II and TEXTOR. A proposal was made to investigate the role of the symmetry

properties of the magnetic field in HSX, where the possibility of performing deuterium plasma experiments will be considered. The isotope effect in regard to an H-mode power threshold has been one of the main issues in the ITPA, so that a link to ITPA activities is to be kept in mind.

3D equilibrium

The validation of HINT2 equilibrium calculations, which has been homework from the 10th CWGM, has progressed in LHD. It has been systematically found that the effective boundary can be identified with the location of the maximum of E_r (radial electric field) shear (deduced from charge-exchange spectroscopy). The peak position of field lines' connection length (HINT2) has been found to fit the peak position of the heat flux to divertor plates (measured by IR camera in collaboration between IPP and NIFS). The plasma response to three-dimensional (3D) magnetic fields will be reported in an invited talk at the 2013 EPS conference (already approved). Also see the previous article in this *Stellarator News*.

Database issues

Extension of the ISHPDB (International Stellarator-Heliotron Profile Database) has been progressing, but some physics topics have had no contributions to the database. A minimum set of magnetic configuration data (VMEC files) has been registered. An interface should be available because VMEC versions may differ from institution to institution.

Extension of the ISHCDB (Confinement Database) towards predictive scaling is mandatory due to different size and shape devices and different operation/parameter regimes. An extended joint EPS2012 paper is now in preparation for publication in *Plasma Physics and Controlled Fusion*.

An extension of the CERC (Core Electron-Root Confinement) collaboration was proposed to include ECH plasmas in HSX, where data from steady-state power balance and perturbative heat transport can be studied in conditions of different degrees of symmetry in the magnetic configuration.

Energetic particles

International collaborations have been successfully developed among TJ-II, LHD, and H-J, making use of data from CHS. The number of joint papers based on joint experiments has steadily increased. There is outreach beyond the stellarator-heliotron (S-H) community through joint experiments conducted in the ITPA Energetic Particle Physics topical group.

The integrated approach, experiment/theory/simulation, was suggested in order to increase the predictive capability on Alfvén eigenmodes and energetic particles properties.

Transport

Significant plasma potential variation on a flux surface, observed in TJ-II ECRH plasmas for the first time, would have an impact on impurity transport under conditions such as HDH (high-density H-mode) in W7-AS and the impurity hole in LHD, through $E_{\text{pol}} \times B$ (radial) drift and parallel impurity transport mechanisms.

The status of a joint IAEA paper on neoclassical transport validation in LHD, TJ-II, and W7-AS was reported. The energy transport studies are to be extended (candidate shots already identified from LHD) through the application of FORTEC-3D.

Development of an integrated transport suite (IPP: predictive, NIFS: experimental analysis) has been progressing. A modular ASTRA-core suite is available at CIEMAT for predictive/interpretative analysis (e.g., the ongoing neoclassical validation activity).

The ion temperature profile obtained by XICS (X-Ray Imaging Crystal Spectrometer) on LHD (a collaboration between PPPL and NIFS) has been incorporated into TASK3D-a suite.

Island dynamics

Recent progress on island experiments in LHD (systematically investigating the plasma parameter and magnetic configuration dependence) and a joint-experiment plan in TJ-II (forcing the appearance of an $\iota = n/m = 4/2$ island with controlled Ohmic induction [where n (m) indicates toroidal (poloidal) mode number] were introduced. Such joint actions will be summarized in presentations planned for the coming ISHW (2013) and IAEA Fusion Energy Conference (2014). Heat pulse propagation experiments (via ECH modulation) in TJ-II jointly with NIFS colleagues, were also reported: instantaneous electron cyclotron emission (ECE) response, associated with ECH pump-out, is found when an $n/m = 3/2$ magnetic resonance reaches certain radial locations. VMEC calculations have been provided at various stages of the calculated evolution of the rotational transform as a basis for 3D equilibrium analysis to be calculated by HINT2.

Link to ITPA

Strengthening of the link between ITPA and CWGM has been continuously promoted. The status of the Integrated Operation Scenario (IOS) topical group was reported, with emphasis on the contributions from the S-H community so far, such as ECH-assisted plasma breakdown and integrated modeling activities.

Recently, the organizational process of SSOCG (Steady State Operations Coordination Group) has progressed by calling for the participation of related IEA (International Energy Agency) Implementing Agreements and national

laboratories. Actively cooled superconducting devices, such as LHD and Wendelstein 7-X in the S-H community, should play leading roles in joint programmes to be formulated.

H-mode

A revision of H-mode phenomenology considering helical devices (W7-AS, CHS, TJ-II, H-J, and LHD) highlighted both the generic nature of the H-mode and its dependence on the 3D magnetic configuration. Therefore, a joint study of the configuration dependence was proposed under the hypothesis, termed "configuration-biased H-mode," that the spin-up of flows to a high-rotation state or the diverse edge instabilities may be biased (or damped) by specific flow conditions in each 3D magnetic configuration. An overview of related data from TJ-II showed a prominent role for low-order rational surfaces in H-mode phenomenology, including bursty activity that might share characteristics with tokamak physics. A wiki page has been setup to launch this joint activity, and details will be announced soon.

The study dedicated to He plasmas (main ion species in the first phase of ITER, where the threshold power is to be studied) was suggested.

Reactor and system code

The HELIAS reactor concept was introduced by emphasizing issues not directly covered by physics optimization for W7-X, as well as technological issues. Pellet fueling has been planned in W7-X to add flexibility to the development of reactor scenarios. It has been found that positive E_r can arise for a hollow density profile, which might contribute to the avoidance of impurity accumulation in the core plasma. Improved and validated physics understanding through the CWGM activity is to be implemented into system codes such as PROCESS and HELIOS.

Highlights in LHD experiment, invitation to joint experiments

Extrapolation of physics in both depth and width has progressed continuously in extended parameter regimes in LHD. The closed divertor works reasonably well (even though only one cryo-pump was installed in the last campaign). Validation of physics models and large-scale computation have been substantially advanced by utilizing well-documented experimental data. 3D effects in toroidal plasmas such as viscosity and topology have been clarified through the cutting-edge capabilities of LHD. Estimates of the effective mass ratio through simultaneous measurement of GAM and Alfvén eigenmodes, and of the He/H ratio through CXRS, have been successfully provided. The schedule of the 17th experiment campaign in FY 2013 was shown to call for joint experiments in LHD. Perspectives

on the further increase of the ion temperature and on the impurity transport study were discussed.

General observations

Throughout the meeting, impurity issues were frequently raised, for which enforced programmatic efforts for intensive research are proposed. In the coming meetings, impurity issues will be extensively treated. Your active participation is anticipated.

The agenda for the 11th CWGM was packed with presentations. This is, of course, a clear sign of progress on a range of topics, on one hand; on the other hand, discussions on programmatic collaboration, such as joint experiments, joint papers, and database activities, were limited. Reflecting this situation, the CWGM format was also discussed. Some ideas were raised, such as the prioritization of topics (e.g., convergence on the stellarator-heliotron reactor proposal), the promotion of session/task leaders to focus on discussion and collaboration-oriented sessions, or the nomination of a “CWGM officer” in each institution. The implementation of some of these ideas will be considered for future CWGMs.

Materials presented at previous CWGMs (except for the first one, unfortunately) can be reached through either the IPP or the NIFS CWGM website (designated at the top of this article). A retrospective look at these materials should be instructive when considering future direction for this activity. A proposal was made to include the technical capabilities of each experimental group in the fusion-wiki.

CWGM12 Announcement

We will be having a short 12th CWGM in Padua Italy at the occasion of the ISHW-RFP Workshop. It will be held in the evening of 20 September (Friday), 2013 at the same venue as the ISHW-RFP Workshop.

The provisional agenda would include:

- ⇒ Progress since CWGM11 (preferably by session leaders in CWGM11)
- ⇒ Brief reports from S-H representatives to ITPA topical groups (if available)
- ⇒ Discussions on joint activities towards 2014 (IAEA-FEC, etc..)

Further details will be made available on the CWGM Web page as the date approaches.

Acknowledgements

We are indebted to Mr. R. Klatt (IPP-Greifswald) for his kind support in making the video-conference possible through EFDA-TV. The 11th CWGM were partly supported by NIFS (National Institute for Fusion Science)/NINS (National Institutes of Natural Sciences) under the project, “Promotion of the International Collaborative Research Network Formation.”

D. López-Bruna (CIEMAT) and M. Yokoyama (NIFS) on behalf of all participants in the 11th CWGM.